

See discussions, stats, and author profiles for this publication at: <https://www.researchgate.net/publication/231683676>

Isothermal morphology diagrams for binary blends of diblock copolymer and homopolymer

ARTICLE *in* MACROMOLECULES · MAY 1992

Impact Factor: 5.8 · DOI: 10.1021/ma00036a014

CITATIONS

155

READS

61

3 AUTHORS, INCLUDING:



[Karen I Winey](#)

University of Pennsylvania

331 PUBLICATIONS 11,291 CITATIONS

SEE PROFILE



[Edwin L Thomas](#)

Rice University

620 PUBLICATIONS 24,408 CITATIONS

SEE PROFILE

Isothermal Morphology Diagrams for Binary Blends of Diblock Copolymer and Homopolymer

Karen I. Winey*[†]

Department of Polymer Science and Engineering, University of Massachusetts, Amherst, Massachusetts 01003

Edwin L. Thomas

Department of Materials Science and Engineering, Massachusetts Institute of Technology, Cambridge, Massachusetts 02139

Lewis J. Fetters

Corporate Research Laboratories, Exxon Research & Engineering Company, Annandale, New Jersey 08801

Received October 30, 1991; Revised Manuscript Received January 25, 1992

ABSTRACT: The equilibrium morphologies observed in over 130 diblock copolymer/homopolymer blends were summarized in two new types of isothermal morphology diagrams. Blends were prepared from homopolystyrene (hPS) and poly(styrene-*b*-isoprene) (SI) or poly(styrene-*b*-butadiene) (SB) diblock copolymer by slow solvent evaporation from a single-phase solution followed by annealing. The isothermal morphology diagrams distinguish the following morphological types: lamellae, the ordered bicontinuous double-diamond morphology, cylinders on a hexagonal lattice, spheres on a cubic lattice, disordered micelles of various shapes, and macrophase separation. The constant molecular weight morphology diagrams illustrated the dependence of the blend morphology on both the copolymer composition and the homopolymer concentration. This style of diagram showed that hPS exhibited a considerably higher solubility limit with a diblock copolymer when the majority component of the copolymer was PS. The constant copolymer composition diagrams emphasized the importance of the relative homopolymer molecular weight and the overall blend composition. These morphology diagrams provide a coherent means by which to present and predict the morphology types in binary blends of amorphous diblock copolymer and homopolymer.

Introduction

The morphologies of a large number of blends containing a diblock copolymer (AB) and a homopolymer (hA) have previously been determined in our laboratory for conditions in which the components A and B are immiscible. Ordered morphologies include lamellae, the ordered bicontinuous double-diamond (OBDD) morphology, cylinders on a hexagonal lattice, and spheres on a cubic lattice as presented elsewhere.¹⁻⁴ Disordered micelles of various shapes have also been observed.^{1,5,6} We present here two types of morphological diagrams to consolidate this information and to provide insight into the morphological transitions.

Current theoretical predictions for AB/hA blends do not account for the extensive variety of observed morphologies. The early theories of AB/hA blends predict the critical micelle concentration (cmc) and the nature of micelles above the cmc but are applicable only at high homopolymer concentrations where micelles do not interact.^{7,8} Theories have also been developed for the onset of long-range order between micelles, but only for the case of spherical micelles.^{9,10} Whitmore and Noolandi's calculations predict the phase behavior of the AB/hA system over the entire homopolymer concentration range as a function of temperature.¹¹ For our purposes, the Whitmore-Noolandi results have two limitations: their theoretical approach is most reliable near the order-disorder transition and only a single morphology, lamellae, is considered.

Experimental phase diagrams have been presented previously by Roe and Zin.¹² These authors constructed temperature versus homopolymer concentration diagrams which delineated macrophase-separated and homogeneous states as determined by cloud-point and SAXS measurements. The SAXS experiments were limited to a few blends containing large fractions of diblock copolymer in which the order-disorder transition was observed. The majority of the phase diagrams by Roe and Zin were constructed from cloud-point measurements which provide no firm evidence of microdomain shape or symmetry and may or may not accurately indicate macrophase separation. Cylindrical micelles in AB/hA blends can be long enough to scatter light, so that samples appear turbid without being macrophase separated.⁵

A binary blend system is fully described by the homopolymer content in the blend, the homopolymer molecular weight, and two parameters to describe the diblock copolymer when the interaction parameter is fixed. The diblock copolymer is defined by two of the following: the molecular weight of block A, the molecular weight of block B, the total molecular weight, and the composition of the diblock copolymer. These molecular parameters are used to construct the morphology diagrams which will assist the development of a comprehensive description of the binary blends of diblock copolymer and homopolymer.

The intermaterial dividing surface is the interface between the A and B microdomains at which the junctions of the copolymers reside. Our previous work with diblock copolymer/homopolymer blends has shown the influence of the homopolymer concentration and the homopolymer molecular weight on the intermaterial dividing surface as characterized by the mean curvature (H) and the average

* To whom correspondence should be addressed.

[†] Current address: AT&T Bell Laboratories, Murray Hill, NJ 07974.

area per copolymer junction (σ_j).^{2,3} The parameters H and σ_j both increase, which indicates a greater extent of mixing between hA and the spatially restricted A block of the copolymer, with increasing homopolymer concentration and with decreasing homopolymer molecular weight. This insight to swelling and mixing in AB/hA blends is used to help interpret our new morphology diagrams.

Experimental Procedures

Materials and Blend Preparation. The anionic polymerization and characterization of poly(styrene-*b*-isoprene) and poly(styrene-*b*-butadiene) diblock copolymers have been described elsewhere.^{1,4} The polydispersity indices for the diblock copolymer are less than 1.05 in all cases. The poly(styrene-*b*-isoprene) and poly(styrene-*b*-butadiene) diblock copolymers are identified as SI*a*/*b* (or IS*a*/*b*) and SB*a*/*b* (or BS*a*/*b*), respectively, where *a* and *b* refer to the block molecular weights given in kilograms per mole and the order of the capital letters indicates the sequence of block synthesis. Table I lists selected characteristics of the SI and SB diblock copolymers. The homopolystyrenes (hPS) were purchased from Pressure Chemical Co. and were designated by their approximate homopolymer molecular weight (in kg/mol) followed by hPS.

The protocol for blend preparation was designed to reproducibly prepare bulk binary blends (~1 mm thick) at thermodynamic equilibrium and was described previously.² Briefly stated, blends were slowly solvent cast from toluene and annealed at 125 °C. Blends are identified by the homopolystyrene concentration in the blend given in weight percent, the homopolystyrene, and the diblock copolymer: 40% 14 hPS and SI27/22.

Transmission Electron Microscopy and Small-Angle X-ray Scattering. Blends were directly imaged with transmission electron microscopy (TEM) to identify the morphology type. Small-angle X-ray scattering was used to further study the morphology of some blends.

We have previously reported four ordered morphologies in AB/hA type blends: lamellae,² the ordered bicontinuous double-diamond morphology,⁴ cylinders on a hexagonal lattice,³ and spheres on a cubic lattice.³ Our results from ordered spherical micelles in AB/hA blends are currently insufficient to distinguish the simple cubic and the body-centered cubic lattices. Disordered micelles have been observed with various shapes: spherical, cylindrical, and lamellar.^{5,6} Partially ordered micelles have also been observed in which the micelles exhibit a preferred nearest-neighbor distance but a poorly defined lattice as evidenced by TEM and SAXS.⁶ The disordering transition discussed here between the ordered morphologies and the disordered micelles is not the order-disorder transition which describes the onset of the homogeneous state in block copolymers upon increasing the temperature and/or decreasing the total molecular weight. In our case, both spatially ordered and spatially disordered micelles are microphase-separated. Finally, we distinguish the macrophase-separated state from the biphasic state as follows: the macrophase-separated state contains two morphologies which have widely different compositions, while the biphasic state contains two ordered morphologies which have similar compositions.

Please refer to the supplemental data of this paper for specific information about the blends included in the following isothermal morphology diagrams.

Constant Molecular Weight Diagrams

Construction of Constant Molecular Weight Diagrams. Constant molecular weight morphology diagrams emphasize the influence of the composition of the copolymer and the homopolymer concentration on the blend morphology. The binary blends of SI diblock copolymers and homopolystyrenes can be fully described by five parameters such as the homopolystyrene molecular weight (M_{hPS}), the SI diblock copolymer molecular weight (M_{SI}), the weight percent of PS in the copolymer (w_{PS}), the weight percent of homopolystyrene in the blend (w_{hPS}), and the interaction parameter. To simplify the analysis, we assume

Table I
Characteristics of the Poly(styrene-*b*-isoprene) and Poly(styrene-*b*-butadiene) Diblock Copolymers

label	M_n (PS)	M_n (total)	PS, wt %	PS, vol %	morphology
SI13/51	12 800	64 200	20	18	cylinders of PS
SI13/34	12 900	46 600	28	25	cylinders of PS
SI27/22	26 600	48 700	55	51	lamellae
IS12/45	45 300	57 500	79	76	cylinders of PI
SB10/23	10 200	33 900	30	27	cylinders of PS
SB40/40	42 300	87 300	48	44	lamellae
SB20/20	20 500	41 000	50	46	lamellae
BS10/23	22 200	31 200	71	67	cylinders of PB
BS10/40	42 000	52 300	80	77	cylinders of PB

the interaction parameter for PS and PI depends only on the temperature. With this assumption, the annealing temperature replaces the interaction parameter as a variable to define the blends in this study. Constant molecular weight diagrams are constructed here for blends having a constant annealing temperature (125 °C), a constant M_{hPS} , and an approximately constant M_{SI} . The two remaining molecular parameters, w_{PS} and w_{hPS} , are the ordinate and abscissa of the plot, respectively. In the limit of zero w_{hPS} , w_{PS} solely determines the morphology of the neat diblock copolymer in the strong segregation limit. A third dimension could be added to the diagram as M_{hPS} , M_{SI} , or the annealing temperature.

Three constant molecular weight morphology diagrams are constructed using the SI diblock copolymers listed in Table I which have an average M_{SI} of 54 300. Figures 1–3 have M_{hPS} = 5900, 14 000, and 36 700, respectively. No blends have been selectively eliminated from these diagrams. A three-dimensional morphology diagram (w_{PS} vs w_{hPS} vs M_{hPS}), in which only M_{SI} and the annealing temperature would be fixed, could be constructed from Figures 1–3. However, the influence of M_{hPS} on the blend morphology is more readily illustrated in the subsequent constant copolymer composition morphology diagrams.

The horizontal lines represent specific blend systems of a hPS and a SI over the entire homopolymer concentration range. The letters near these lines indicate the observed microstructure as defined in the figure caption. Blends exhibiting partially ordered micelles are indicated with filled symbols, and biphasic regions are denoted by a diagonal line within the square. The critical micelle concentration, i.e., the w_{hPS} above which micelles do not exist, is not included in these morphology diagrams and is probably greater than 98% hPS.¹

Discussion of Constant Molecular Weight Morphology Diagrams. Blends with a lamellar diblock copolymer and a homopolystyrene produce a larger variety of microstructures than blends with a cylindrical diblock copolymer having either PS or PI cylinders and a homopolystyrene. Blends of 6 hPS or 14 hPS and SI27/22 (w_{PS} = 55%) exhibit multiple-ordered morphologies as the homopolymer content in the blend increases. Only in one case does a cylindrical diblock copolymer exhibit an ordered morphology other than that of the neat diblock copolymer. The intermaterial dividing surface of a lamellar diblock copolymer, unlike cylindrical diblock copolymers, can be readily manipulated by the addition of homopolymer into shapes highly perturbed from its original planar state. A single lamellar diblock copolymer and various homopolymers are capable of producing a variety of morphologies by blending, as opposed to synthesizing separate diblock copolymers for each desired morphology.³

As w_{hPS} increases further, micelles with long-range order undergo a transition to micelles with liquid-like order. This

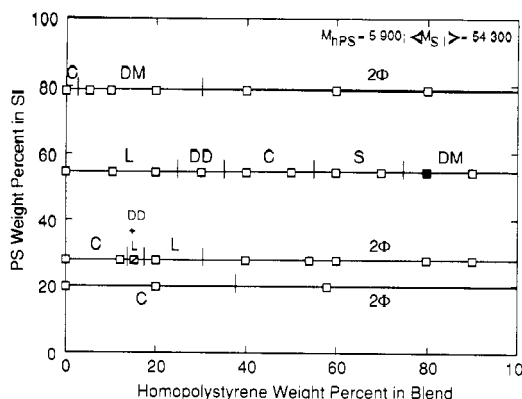


Figure 1. Constant molecular weight morphology diagram for homopolystyrene of 5900 and poly(styrene-*b*-isoprene) diblock copolymers of $\sim 54\,000$. Letters on this and all other figures indicate the morphology: DM, disordered micelles; S, spheres on a cubic lattice; C, cylinders on a hexagonal lattice; DD, the ordered bicontinuous double-diamond morphology; L, ordered lamellae; 2Φ , macrophase separation. Filled symbols indicate blends with partial order.

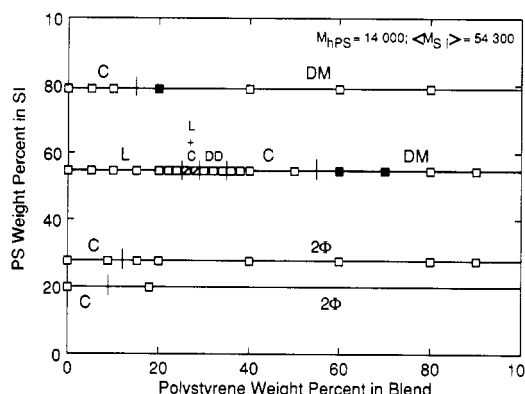


Figure 2. Constant molecular weight morphology diagram for homopolystyrene of 14 000 and poly(styrene-*b*-isoprene) diblock copolymers of $\sim 54\,000$.

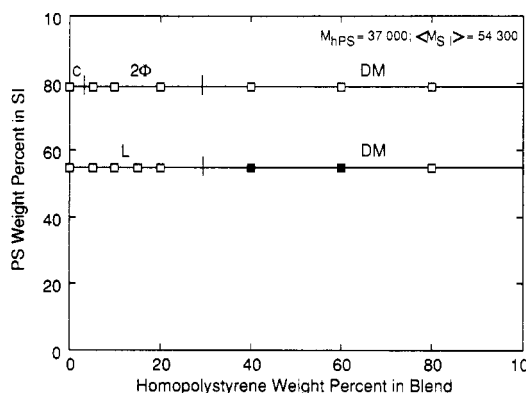


Figure 3. Constant molecular weight morphology diagram for homopolystyrene of 36 700 and poly(styrene-*b*-isoprene) diblock copolymers of $\sim 54\,000$.

transition occurs at lower w_{hPS} as w_{PS} increases. For example, blends of 14 hPS and SI27/22 ($w_{\text{PS}} = 55\%$) disorder (from cylinders on a hexagonal lattice to cylindrical micelles) between 50% and 60% hPS, while blends of 14 hPS and SI12/45 ($w_{\text{PS}} = 79\%$) disorder (from cylinders on a hexagonal lattice to spherical micelles) between 10% and 20% hPS; see Figure 2. Similarly, blends with 6 hPS disorder at $w_{\text{hPS}} = 70\text{--}80\%$ for $w_{\text{PS}} = 55\%$ and at $w_{\text{hPS}} = 20\text{--}40\%$ for $w_{\text{PS}} = 79\%$; see Figure 1.

Diblock copolymer micelles order to minimize the corona-corona overlap, thus reducing the repulsive interaction. [The corona is the region within a micelle which

contains homopolymers, hA, and the A blocks of the copolymers; the core refers to the region within a micelle which contains the B blocks of the copolymers.] This argument applies to blends having a homopolymer molecular weight comparable to or less than the block molecular weight. The addition of homopolymer sufficiently screens the repulsive interactions between the coronas. As shown above, less homopolymer is required to produce this screening effect when the homopolymer is added to the matrix component of a cylindrical diblock copolymer as compared to a lamellar diblock copolymer. Restated in terms of the molecular parameters, the homopolymer concentration over which disordered micelles are observed increases as w_{PS} increases at fixed M_{hPS} and M_{SI} .

Limited homopolystyrene solubility predominates in blends containing diblock copolymer with low w_{PS} . This is the case even when M_{hPS} is significantly smaller than the PS block molecular weight. Macrophase separation occurs as the solvent evaporates in the presence of even a modest amount of 6 hPS or 14 hPS with diblock copolymers containing PS cylindrical microdomains, SI13/51 ($w_{\text{PS}} = 20\%$) or SI13/34 ($w_{\text{PS}} = 28\%$); see Figures 1 and 2. Typically, homopolystyrene penetrates the cylindrical domains to a small degree ($\sim 5\%$) as w_{hPS} increases before macrophase separating at the homopolymer solubility limit. Only in the case of 6 hPS and SI13/34 is the presence of homopolymer capable of causing a morphological transition to an ordered morphology other than cylinders (see Figure 1). Higher homopolymer concentrations of 6 hPS with SI13/34 produce macrophase separation in which one phase has a high hPS content and the second phase exhibits lamellar micelles.

The diblock copolymers having $w_{\text{PS}} < 50\%$ must form inverted phases to accommodate larger quantities of homopolymer without the onset of macrophase separation. Inverted morphologies result from the swelling of the minority block of the copolymer to such an extent that its effective volume per chain is larger than that of the unswollen majority block of the copolymer.⁴ Such extensive swelling is favored by the entropy of mixing and is limited by the chain stretching of the minority block. The observation of macrophase separation upon increasing w_{hPS} in blends with $w_{\text{PS}} < 50\%$ indicates the extension of the minority block of the copolymer is indeed limited. Macrophase separation may also occur in part because of the translational entropy loss from the confinement of homopolymer within microdomains of comparable size. Though the exact positions of the macrophase-separation transitions are not established by this study, the homopolymer concentration range for macrophase separation generally increases as w_{PS} decreases at fixed M_{hPS} and M_{SI} .

Biphasic regions as a function of composition are characteristic of first-order phase transitions in two-component blends. A biphasic region in which two ordered morphologies coexist is expected at homopolymer concentrations between the regions of single ordered morphologies. We have not yet observed such systematic biphasic regions. Typically, biphasic regions are absent or, if present, contain unexpected combinations of two ordered morphologies. For blends of 14 hPS and SI27/22 ($w_{\text{PS}} = 55\%$), the absence of an observed biphasic region between the OBDD morphology and cylinders indicates that the true biphasic region is quite narrow ($w_{\text{hPS}} < 2\%$). A biphasic region of lamellae and cylinders is observed between lamellae and the OBDD morphology at $w_{\text{PS}} = 55\%$ and $M_{\text{hPS}} = 14\,000$ (Figure 2). This biphasic region

has been confirmed by small-angle X-ray scattering, where peaks for both a lamellar and a hexagonal lattice coexist. The constant molecular weight diagram with 6 hPS (Figure 1) shows an OBDD morphology and lamellar biphasic region between cylinders and lamellae. This example might imply the presence of a very narrow region of the OBDD morphology and the accompanying biphasic region (OBDD morphology and cylinders) between the observed regions of single morphologies. The energy differences between the morphologies near the transitions are quite small, so that the observed metastable morphologies may be kinetically controlled. We currently do not have a satisfactory explanation for the peculiar ordered biphasic results.

Constant Copolymer Composition Diagrams

Construction of Constant Copolymer Composition Diagrams. While the constant molecular weight morphology diagrams focus on the influence of the composition of the copolymer, the constant copolymer composition morphology diagrams feature the influence of the homopolymer molecular weight. The five molecular parameters to describe the binary blends of SI or SB diblock copolymer and homopolystyrene are as before, except that the PS block molecular weight of the copolymer ($M_{\text{PS block}}$) has been substituted for the total diblock copolymer molecular weight. The annealing temperature is held constant at 125 °C, as before, and w_{PS} is held approximately constant. In order to accommodate diblock copolymers with slightly different w_{PS} , the horizontal axis is the overall polystyrene volume fraction (Φ_{PS}) instead of w_{hPS} . The overall PS volume fraction has been identified as an important parameter in binary blends^{3,4} and is paramount for determining the morphology of neat diblock copolymers.^{13,15} The two remaining parameters, M_{hPS} and $M_{\text{PS block}}$, are combined into the relative homopolymer molecular weight, $M_{\text{hPS}}/M_{\text{PS block}}$, and plotted on the vertical axis. This reduced parameter characterizes the extent of mixing between the hPS and the spatially restricted PS block. Using a relative molecular weight implies the absolute molecular weights of the blend system are not relevant which is reasonable within the relatively small range of molecular weights used in this study. A third dimension could be added to the diagram as w_{PS} or the annealing temperature.

Figure 4a shows the constant copolymer composition diagram for lamellar diblock copolymers with a composition range of $f = 44\text{--}51\text{ vol \% PS}$, where f is the polystyrene volume fraction in the neat diblock copolymer. Note that the location and groupings of the morphologies of all 83 blends are consistent and no blends have been selectively removed. Sixteen of these blends were prepared by Kinning using the same protocol.^{1,5} The shape of the symbol indicates the specific diblock copolymer used in the blends, and the lower limits in Φ_{PS} equal the compositions of the neat diblock copolymers; see Table I. Solid lines indicate the boundaries between ordered morphologies, and dashed lines indicate boundaries between the spatially ordered morphologies and spatially disordered micelles. These lines we have drawn to separate different morphologies on the diagram are not very precisely located due to limited experimental data. The critical micelle concentration occurs at very large PS volume fractions for these blends and is not indicated on this morphology diagram. Figure 4b shows the same morphology diagram without the experimental data.

Discussion of Constant Copolymer Composition Diagrams. The constant copolymer composition mor-

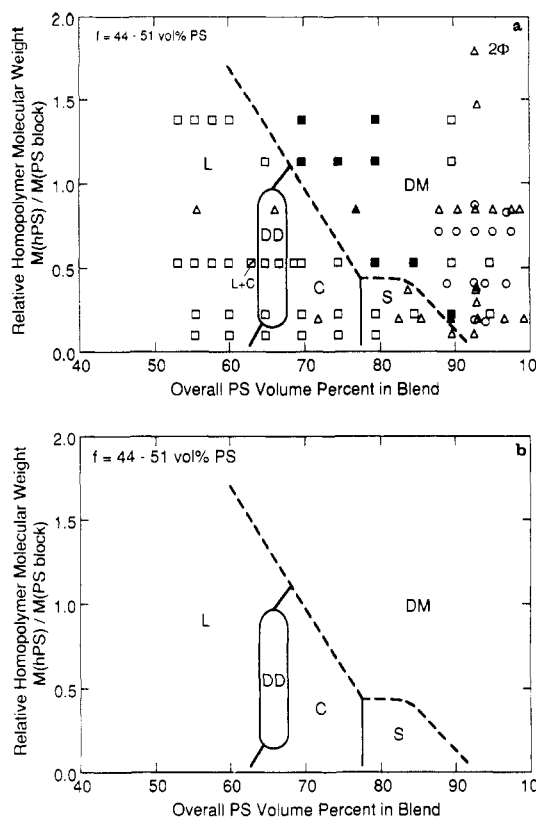


Figure 4. (a) Constant copolymer composition morphology diagram for various homopolystyrenes blended with lamellar diblock copolymers of $f = 44\text{--}51\text{ vol \% PS}$: (\square) SI27/22, (Δ) SB20/20, (\circ) SB40/40. Solid lines indicate the boundaries between ordered morphologies, and dashed lines indicate the boundary between spatially ordered micelles and spatially disordered micelles. (b) The constant copolymer composition morphology diagram from part (a) shown without the data.

phology diagram for lamellar diblock copolymers blended with homopolystyrene illustrates the morphological versatility of lamellar diblock copolymers presented previously in the context of constant molecular weight morphology diagrams. The relative homopolymer molecular weight and Φ_{PS} are well-chosen parameters and give consistent results for poly(styrene-*b*-isoprene) and poly(styrene-*b*-butadiene) diblock copolymers. In particular, Φ_{PS} unifies the morphological data for diblock copolymers with slightly different w_{PS} in contrast to using w_{hPS} . For example, the blend of 30% 14 hPS and SI27/22 ($w_{\text{PS}} = 55\%$) and the blend of 40% 17 hPS and SB20/20 ($w_{\text{PS}} = 50\%$) both exhibit the ordered bicontinuous double-diamond morphology, where Φ_{PS} varies by only 1% though w_{hPS} varies by 10%. The ordered biphasic region of lamellae and cylinders (L + C), as discussed with respect to the constant molecular weight morphology diagram, is the only biphasic region observed for binary blends of lamellar diblock copolymers and homopolymers.

The sequence of order-order morphological transitions with increasing Φ_{PS} depends on the relative homopolymer molecular weight. Increasing Φ_{PS} in the blend at $M_{\text{hPS}}/M_{\text{PS block}}$ below ~ 0.15 successively yields lamellae, cylinders on a hexagonal lattice, spheres on a cubic lattice, and disordered micelles. Values at $M_{\text{hPS}}/M_{\text{PS block}} \approx 0.15\text{--}1.0$ produce a succession of lamellae, the OBDD morphology, cylinders on a hexagonal lattice, spheres on a cubic lattice, and disordered micelles or a succession of lamellae, the OBDD morphology, hexagonally ordered cylinders, and disordered micelles as Φ_{PS} increases. The absence of an ordered regime of spheres above $M_{\text{hPS}}/M_{\text{PS block}} \approx 0.4$ is due to the intervening disordering of the

cylindrical micelles at a lower Φ_{PS} in the blend. At $M_{hPS}/M_{PS\text{ block}} > 1.0$, the lamellar morphology spatially disorders to a combination of disordered lamellar and cylindrical micelles upon the addition of homopolymer prior to any order-order transitions.

The vertical lines between the ordered morphologies in the constant copolymer composition morphology diagram are in approximate agreement with the PS volume percent boundaries established for the pure SI diblock copolymers in the strong segregation limit, namely: lamellae, 33–62 vol % PS; the OBDD morphology, 62–66 vol % PS; cylinders, 66–77 vol % PS; spheres on a body-centered cubic lattice, ≥ 77 vol % PS.^{16,17} Similarly, if a binary blend is ordered, the value of Φ_{PS} is sufficient to determine the morphology type, except for the blends with approximately 65 vol % PS. The ordered morphologies of these blends depend on both Φ_{PS} and $M_{hPS}/M_{PS\text{ block}}$. At $\Phi_{PS} = 65\%$, the ordered morphology type changes from hexagonally packed cylinders to the OBDD morphology to lamellae before losing long-range order upon increasing the relative homopolymer molecular weight. The OBDD morphology is observed in binary blends with ~ 65 vol % PS and $0.15 < M_{hPS}/M_{PS\text{ block}} < 1.0$. Though on our diagram we have not distinguished between spherical, cylindrical, and lamellar disordered micelles, the TEM results indicate micellar shape changes upon increasing the relative homopolymer molecular weight. For example, blends prepared with SB40/40 exhibit the following morphologies at $\Phi_{PS} = 93\%$: disordered spherical micelles at $M_{hPS}/M_{PS\text{ block}} = 0.18$ and 0.41 , disordered cylindrical micelles at $M_{hPS}/M_{PS\text{ block}} = 0.71$, disordered lamellar micelles at $M_{hPS}/M_{PS\text{ block}} = 0.87$. Similar results have been reported by Kinning et al.^{1,5}

The mean curvature (H) of the PS-PI interface and the average area per copolymer junction (σ_j) were calculated for the blends containing SI27/22 using the lattice parameter determined via SAXS and Φ_{PS} .³ Note that, in all cases, we have defined the mean curvature of the intermaterial dividing surface as positive toward the PI microdomain, and an increase in H indicates a more highly convex polyisoprene surface. H and σ_j generally increase or remain constant as $M_{hPS}/M_{PS\text{ block}}$ decreases or Φ_{PS} increases. These trends are typically observed both within and between ordered morphology types. These trends have also been demonstrated in disordered spherical micelles.³ Decreasing the relative homopolymer molecular weight in the blend increases the degree of swelling in the PS block which perturbs the PS-PI interface to a greater extent and promotes the lateral separation of the copolymer molecules as evidenced by an increase in H and σ_j , respectively. Increasing w_{hPS} or Φ_{PS} increases the swelling of the PS block until the PS block is saturated. Further addition of hPS screens the corona-corona interactions causing the microdomains to spatially disorder. Increased swelling of the PS block due to the presence of homopolymer increases the mean curvature of the PS-PI interface and the area per copolymer junction within the ordered morphologies.

The loss of long-range order depends on $M_{hPS}/M_{PS\text{ block}}$ and Φ_{PS} as illustrated by the constant copolymer composition diagram. The onset of liquid-like order exhibits a slope of approximately -0.05 for spherical micelles at $M_{hPS}/M_{PS\text{ block}} < 0.4$. A negative slope is also observed for the spatial disordering of cylindrical and lamellar micelles though the slope of these lines are not as well defined by the present data. The OBDD morphology does not exhibit a disordering transition. The minority component of the OBDD morphology consists of two interpenetrating net-

works of diamond symmetry which apparently change shape to cylinders prior to (or perhaps during) the loss of long-range order.

A negative slope for the onset of liquid-like order can be understood in terms of corona thickness and corona-corona interactions. Kinning et al. found the corona thickness of disordered spherical micelles increases as the homopolymer molecular weight decreases.¹ Smaller molecular weight homopolymers penetrate and mix with the spatially constrained blocks of the copolymers to a greater extent than larger homopolymer molecules. Consequently, the smaller molecular weight homopolymers produce a thicker corona, with the homopolymer distributed approximately uniformly throughout the corona. In contrast, higher molecular weight homopolymers create a thinner corona region in which the homopolymers partially segregate outside the corona. This high homopolymer concentration between micelles more effectively screens the micelle-micelle interactions. A smaller weight fraction of high molecular weight homopolymer is thus required to fully screen the corona-corona interactions and to induce liquid-like order, as compared to the low molecular weight homopolymer. Therefore, at higher $M_{hPS}/M_{PS\text{ block}}$ a smaller Φ_{PS} is required to spatially disorder micelles. This results in a negative slope for the transition from long-range order to short-range order within the constant copolymer composition morphology diagram.

The dashed line demarking the loss of long-range order undergoes an abrupt shift to lower Φ_{PS} between spherical micelles on a cubic lattice and cylinders on a hexagonal lattice. This discontinuity in the onset of liquid-like order for spherical and cylindrical micelles arises due to the different packing efficiencies for spheres and long cylinders. Micelles will begin to spatially disorder approximately when the micellar coronas are no longer in contact, that is, when the micellar volume fraction falls below a critical value. The micellar volume fraction includes the volume of the micellar cores and coronas, in contrast with the overall PS volume fraction, which includes the volume of the corona and matrix. The critical micellar volume fraction (here taken as the volume occupied by just-touching micelles) depends on the shape of the packing motif and the lattice type as illustrated here: 52% for spheres on a simple cubic lattice, 68% for spheres on a body-centered cubic lattice, and 91% for cylinders on a hexagonal lattice. Thus, long cylinders require a significantly higher micellar volume fraction to fully order than spheres regardless of the particular lattice of the ordered spheres. The micellar volume fraction decreases as w_{hPS} or Φ_{PS} increases, so that a lower volume of Φ_{PS} is required to spatially disorder cylinders on a hexagonal lattice as compared to spheres on a cubic lattice.

Two additional constant copolymer composition morphology diagrams, Figures 5 and 6, are presented using copolymers which have copolymer compositions in the range of $f = 25$ –27 vol % PS (polystyrene cylinders in a polydiene matrix) and $f = 68$ –77 vol % PS (polydiene cylinders in a polystyrene matrix), respectively. These morphology diagrams are constructed from a smaller number of AB/hA blends and are subsequently more qualitative. The most noteworthy feature of Figures 5 and 6 is the limited presence of ordered morphologies other than that of the neat diblock copolymer. As illustrated previously by the constant molecular weight morphology diagrams, lamellar diblock copolymers produce a greater variety of morphologies when blended with homopolymers than cylindrical diblock copolymers blended with homopolymers.

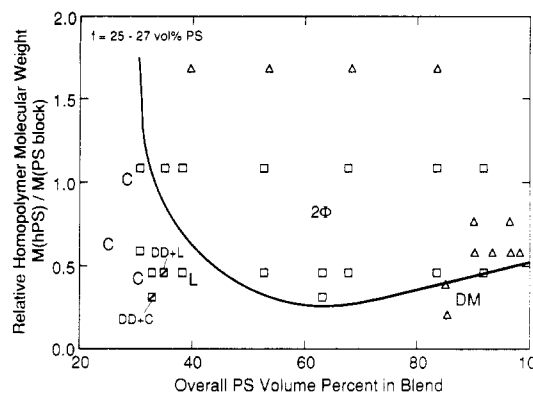


Figure 5. Constant copolymer composition morphology diagram for various homopolystyrenes blended with cylindrical diblock copolymers of $f = 25\text{--}27$ vol % polystyrene: (\square) SI13/34 and (Δ) SB10/23. The solid line denotes the region of macrophase separation in the binary blends.

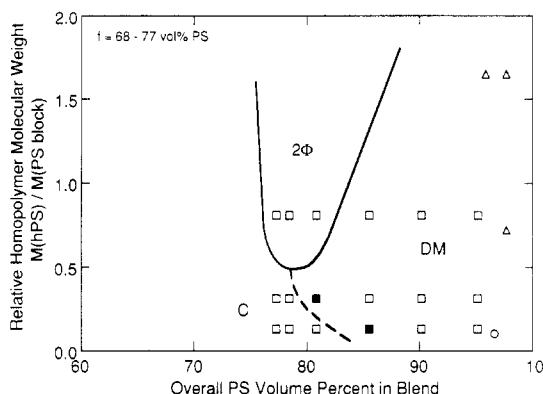


Figure 6. Constant copolymer composition morphology diagram for various homopolystyrenes blended with cylindrical diblock copolymers of $f = 68\text{--}77$ vol % polystyrene: (\square) IS12/45, (Δ) BS10/40, and (\circ) BS10/23. The solid line denotes the region of macrophase separation, and the dashed line denotes the boundary between ordered and disordered micelles.

Figure 5 exhibits the extensive macrophase-separation behavior which occurs when a homopolymer is blended with the minority component of a diblock copolymer. The macrophase-separation region extends to a relative homopolymer molecular weight of less than 0.5 and spans an overall polystyrene volume percent of 35–100%. The macrophase-separation region of Figure 6, which summarizes the resultant morphologies of blending a homopolymer with the majority component of a diblock copolymer, reaches the $M_{hPS}/M_{PS \text{ block}}$ value of 0.7 but is narrow in the overall PS volume percent in the blend. Together these diagrams for cylindrical diblock copolymers extend the constant copolymer composition morphology diagram for lamellar diblock copolymers (Figure 4) in the third dimension to both lower and higher copolymer compositions. The region of macrophase separation in AB/hA blends enlarges dramatically as the copolymer composition becomes more asymmetric. Similar comparisons between Figures 4–6 can be made with respect to the region of disordered micelles. These preliminary results for the

copolymer composition dependence of the constant copolymer composition diagram indicate that a large number of copolymer compositions would have to be studied before a detailed three-dimensional morphology diagram could be constructed.

Conclusions

Isothermal morphology diagrams provide a succinct and insightful means for identifying the morphologies of binary blends and for evaluating the interactions between diblock copolymers and homopolymers. We anticipate that the trends present in these constant molecular weight and the constant copolymer composition morphology diagrams are general features of AB/hA type blends of amorphous polymers. Both types of diagrams illustrate the morphological transitions between ordered morphologies as well as the loss of long-range order. Screening of the corona–corona interactions is promoted by increasing the homopolymer molecular weight and/or the homopolymer concentration.

Acknowledgment. This work was supported by Grant NSF-DMR 89-07433. K.I.W. received support through a NSF Graduate Fellowship and a University of Massachusetts Fellowship.

Supplementary Material Available: Tables of data on constant molecular weight diagrams with 6 hPS and SI, 14 hPS and SI, and 37 hPS and SI and of data on constant copolymer composition diagrams with $f = 25\text{--}27$, 44–51, and 68–77 vol % PS (8 pages). Ordering information is given on any current masthead page.

References and Notes

- (1) Kinning, D. J.; Thomas, E. L.; Fetters, L. J. *J. Chem. Phys.* **1989**, *90*, 5806.
- (2) Winey, K. I.; Thomas, E. L.; Fetters, L. J. *Macromolecules* **1991**, *24*, 6182.
- (3) Winey, K. I.; Thomas, E. L.; Fetters, L. J. *J. Chem. Phys.* **1991**, *95*, 9367.
- (4) Winey, K. I.; Thomas, E. L.; Fetters, L. J. *Macromolecules* **1992**, *25*, 422.
- (5) Kinning, D. J.; Winey, K. I.; Thomas, E. L. *Macromolecules* **1988**, *21*, 3502.
- (6) Winey, K. I.; Thomas, E. L.; Fetters, L. J., to be submitted for publication.
- (7) Leibler, L.; Orland, H.; Wheeler, J. C. *J. Chem. Phys.* **1983**, *79*, 3550.
- (8) Mayes, A. M.; Olvera de la Cruz, M. *Macromolecules* **1988**, *21*, 2543.
- (9) Leibler, L.; Pincus, P. A. *Macromolecules* **1984**, *17*, 2922.
- (10) Semenov, A. N. *Macromolecules* **1989**, *22*, 2849.
- (11) Whitmore, M. D.; Noolandi, J. *Macromolecules* **1985**, *18*, 2486.
- (12) Roe, R.-J.; Zin, W.-C. *Macromolecules* **1984**, *17*, 189.
- (13) Helfand, E.; Wasserman, Z. R. In *Developments in Block Copolymers—I*; Goodman, I., Ed.; Applied Science: New York, 1982.
- (14) Semenov, A. N. *Sov. Phys. JETP* **1985**, *61*, 733.
- (15) Ohta, T.; Kawasaki, K. *Macromolecules* **1986**, *19*, 2621.
- (16) Hasegawa, H.; Tanaka, H.; Yamasaki, K.; Hashimoto, T. *Macromolecules* **1987**, *20*, 1651.
- (17) Gobran, D. A. Ph.D. Dissertation Thesis, University of Massachusetts, Amherst, MA, 1990.

Registry No. hPS (homopolymer), 9003-53-6; SI (block copolymer), 105729-79-1; SB (block copolymer), 106107-54-4.